Journal of Biomechanics 104 (2020) 109713

Contents lists available at ScienceDirect

Journal of Biomechanics

journal homepage: www.elsevier.com/locate/jbiomech
www.JBiomech.com

Exploring the regional disc bulge response of the cervical porcine intervertebral disc under varying loads and posture

Kayla M. Fewster [a], Mamiko Noguchi [a], Chad E. Gooyers [a,b], Alexander Wong [c], Jack P. Callaghan [a,*]

[a] Department of Kinesiology, University of Waterloo, Waterloo, ON, Canada
[b] Department of Systems, 30 Forensic Engineering, Toronto, Ontario, Canada
[c] Department of Systems Design Engineering, University of Waterloo, Waterloo, ON, Canada

ARTICLE INFO

Article history:
Accepted 18 February 2020

Keywords:
Intervertebral disc
Bulging
Laser scanner
Annulus fibrosus

ABSTRACT

Nerve compression due to intervertebral disc (IVD) bulging is a known mechanism for low back pain and typically occurs in the posterior region of the disc. Most *in vitro* studies are limited in the ability to quantify the magnitude of bulging on the posterior aspect of the disc due to the boney structures that occlude a direct line-of-sight in the intact functional spinal units (FSUs). This study examined anterior and posterior annulus fibrosus (AF) bulges in reduced (posterior elements removed) cervical porcine specimens across four loading conditions and two postures. Surface scans from the anterior and posterior aspect of the IVD were recorded in both neutral and flexed postures using a 3D laser scanner to characterize changes in AF bulge. A significant negative correlation was observed for peak AF bulge on the anterior and posterior side of the disc in a flexed posture (Pearson's $r = -0.448$; $p = 0.002$; $r^2 = 0.2003$). The results from this investigation support that there may be a connection between the magnitude of AF bulge on the posterior side and estimations computed using the anterior side.

1. Introduction

Intervertebral disc (IVD) bulging is a known mechanism for low back pain due to compression of the spinal cord in the spinal canal or impingement of the spinal nerve roots in the neural foramina (Brinckmann et al., 1989; Cuchanski et al., 2011; Stokes, 1988; Wenger and Schlegel, 1997). This mechanism of injury typically occurs in the posterior region of the disc and is characterized by the migration of the nucleus through the annulus (Haughton, 1988; Tampier et al., 2007). There are only a few studies that have quantified the magnitude of bulging on the posterior aspect of the disc. This is likely attributable to bony structures and passive tissues that occlude a direct line-of-sight to the posterior-lateral region of intact functional spinal units (FSUs).

Previous research by Heuer and colleagues (2008a) has characterized the effect of posture on IVD bulging on human lumbar FSUs. With the posterior elements of the FSUs removed, results from this investigation revealed that among various single axis and combined loading conditions, the highest IVD bulge was observed when 7.5 Nm flexion moment was applied (Heuer et al., 2008a). However, to the best of the author's knowledge, the combined effects of increasing magnitudes of compressive load and posture on IVD bulging have yet to be investigated.

Therefore, to better understand how the behavior of the anterior portion of the IVD may be related to the posterior-lateral region, this study quantified the magnitude of anterior and posterior-lateral bulge in the IVD across different posture conditions and magnitudes of compressive load. In-line with this objective, it was hypothesized that a negative correlation between anterior and posterior bulging would emerge. Results from this study may elucidate a link between loading type (compressive load and posture) and IVD bulge on the anterior side of an FSU that would facilitate inferences on the structural changes in the posterior-lateral regions of intact specimens.

2. Methods

2.1. Specimen preparation

Twelve FSUs (6 C3-C4, 6 C5-C6) were obtained from six porcine cervical spines. Each FSU included the IVD and two adjacent vertebral bodies at the level of c34 and c56. All cervical spine specimens were obtained following death and stored frozen at −20 °C. Porcine cervical FSUs were used as surrogates for the human lumbar

* Corresponding author at: Faculty of Applied Health Science, Department of Kinesiology, University of Waterloo, Waterloo, ON N2L 3G1, Canada.
E-mail address: jack.callaghan@uwaterloo.ca (J.P. Callaghan).

https://doi.org/10.1016/j.jbiomech.2020.109713
0021-9290/

spine due to their anatomical and functional similarities (Oxland et al., 1991; Yingling et al., 1999). Prior to testing, specimens were thawed at room temperature for 12 h. Dissection included isolating the two FSUs and removing the surrounding musculature, leaving only the osteoligamentous structures intact. Once dissection was complete, the locations of the cartilaginous endplates on the anterior surface of the FSU were marked with three steel pins (0.5 mm diameter; 6 per specimen). One pin was placed at the center of the IVD, while the remaining two pins were placed on the anterolateral sides (Fig. 1). The purpose of the inserted pins was to align the 3D surface profiles from each FSU and estimate the curvature of the endplate. Next, the superior and inferior vertebrae of the FSU were fixed using custom-machined aluminum cups using a combination of wood screws and dental plaster.

2.2. Procedure

Once potted, specimens were mounted in a modified servo-hydraulic materials testing system (Model 8872; Instron, Canton, MA, USA). The lower vertebra of each specimen was free to translate in the anterior–posterior direction (via bearing tray), which enabled the centre of rotation to translate within the joint during testing, ensuring compressive loading was in line with the centre of rotation (Callaghan and McGill, 2001). Each FSU first received a 15-minute preload consisting of 300 N of static compressive load (under load control) to counter postmortem swelling (Callaghan and McGill, 2001). During this preload, an independent servomotor (AKM23D; Kollmorgen/Danaher Motion, Radford, VA, USA) connected in-series with a torque cell (T120-106-1K; SensorData Technologies Inc., Sterling heights, MI, USA) was used to establish and identify the position of minimal stiffness for the specific FSU. Following preload, three cycles of passive flexion-extension was completed. While under 300 N of compressive load, FSUs were rotated about the flexion-extension axis, at a rate of 0.5 degrees per second, until an ±8 Nm moment was reached. This test was completed to identify the limits of each FSUs neutral zone. Throughout testing, the applied moment and angular displacement were continuously sampled at 25 Hz. Flexion and Extension neutral zone limits were then identified using methods described by Thompson et al. (2003).

Similar to previous work within our group, a 2D laser displacement sensor (LJ-V7080, Keyence Corporation, Osaka, Japan) was used to characterize the anterior surface profile of the IVD (Gooyers and Callaghan, 2015). Surface profiles were characterized across four levels of compressive load (10 N, 300 N, 600 N and 1200 N) and two posture conditions (Neutral and Flexion). The neutral posture was defined as the center of the neutral zone. The flexion posture was defined as 300% of the flexion neutral zone limit. This limit was designed to bring the isolated FSU to the end of its natural physiological range (i.e., where the passive rotational stiffness begins to deviate from linear). The laser displacement sensor (Fig. 2) was mounted on a 48-cm linear guide (NSK Ltd., Tokyo, Japan) and interfaced with a linear encoder (LS 328-C, Heidenhain, Schaumburg, IL, USA) to obtain a 3D cross-sectional scan of the IVD surface of the FSU every 40 μm in the frontal plane (Gooyers and Callaghan, 2015). Manufacturer's specifications indicated that the laser displacement sensor had an accuracy of 46 μm in the transverse direction (i.e., primary bulge axis) and resolution of 20 μm in the vertical direction (Gooyers and Callaghan, 2015). Each scan was recorded in less than fifteen-seconds.

This study used a randomized block design; posture was blocked by load and a balanced block design was used for image location. Once the anterior aspect of the FSU was scanned throughout all conditions with the posterior elements intact (i.e., Anterior-Intact), the FSU was removed from the testing system and the posterior elements of the specimen were removed. This involved dissecting out the spinous process by cutting through the pedicles, as well as dissecting out the posterior longitudinal ligament to expose the posterior aspect of the IVD for surface profile scanning. This left a reduced FSU. The specimen was then re-mounted in the servo-hydraulic testing device and the anterior and posterior sides of the IVD were scanned during all remaining conditions (anterior-reduced and posterior). The order in which each side of the reduced FSU was scanned (anterior-reduced vs. posterior) was randomized across specimens. For both Intact and Reduced conditions, the same Flexed and Neutral postures (in degrees) were used for consistency and comparisons of Anterior-Intact and Anterior-Reduced. Prior to the commencement of scanning within each condition (Anterior-Intact, Anterior-Reduced, and Posterior) a neutral scan was captured (neutral posture with 10 N load) to facilitate laser image alignment. In addition to the three neutral scans, a total of 24 scans (load x4, posture x2, and scan location x3) were collected from each specimen.

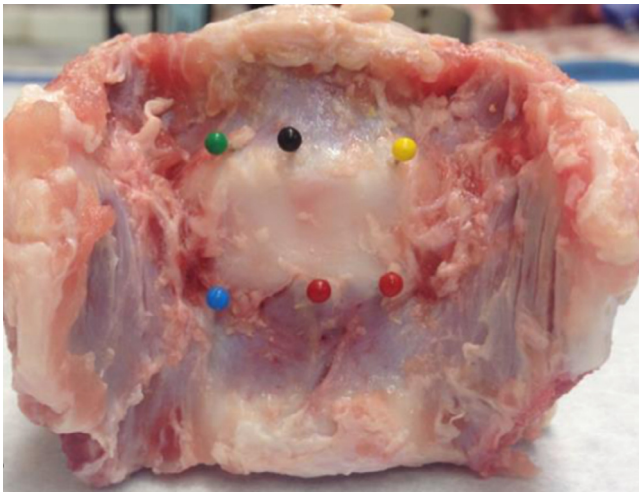

Fig. 1. Three steel pins were inserted into the superior and inferior cartilaginous endplates to facilitate registration of the 3D surface scans across conditions. Note that the pin heads have not yet been removed to enhance visibility for the figure but were not present for scanning.

2.3. Data processing

IVD profile data from the laser scans were processed in MATLAB (version R2015b, Mathworks, Natick, MA). Each 2D vertical scan was captured every 40 μm along the anterior surface of the FSU (i.e., a total number of scans in the frontal plane, M) and was "stitched together" to create an Mx800 data matrix (Gooyers and Callaghan, 2015). All surface profile data collected for each specimen were first aligned in order to account for any translation that may have occurred with respect to the laser. The endplate surface curvature was reconstructed based on the location of the inserted steel pins (Fewster et al., 2019). Peak AF bulge (inward or outward) was determined with respect to the reconstructed endplate surface curvature, using a newly developed algorithm (Fewster et al., 2019) (Fig. 3).

2.4. Statistical analyses

Due to technical difficulties with the laser system, one FSU was excluded, resulting in a total of 11 specimens that were included in this study. To determine whether the removal of posterior elements had an effect on peak AF bulge, a paired *t*-test was employed to compare Anterior-Intact and Anterior-Reduced peak AF bulge measurements. To determine if there was a relationship between

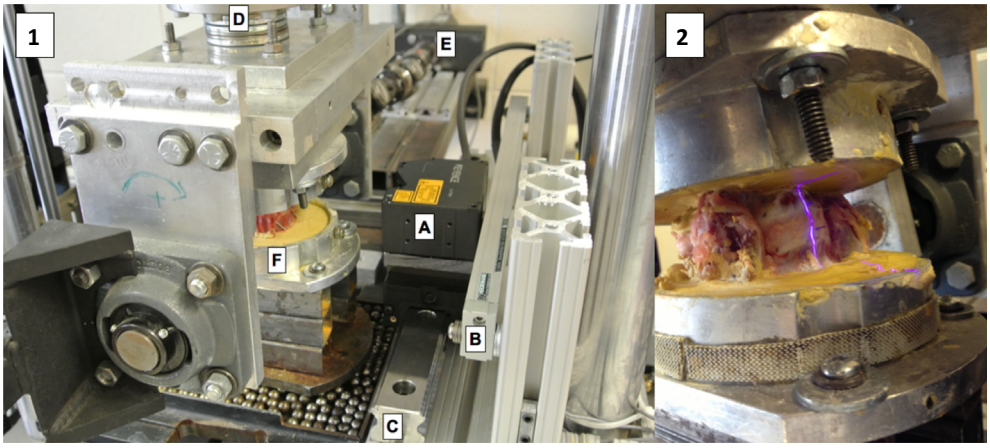

Fig. 2. (1) The modified testing apparatus consisting of: (A) 2D laser head, (B) linear encoder, (C) linear guide, (D) load cell in-line with Instron actuator, (E) flexion/extension torque motor, and (F) FSU potted in aluminium cups with dental plaster. (2) FSU potted in custom-machined aluminum cups and mounted in the modified testing system with the visible laser on the anterior surface of the FSU.

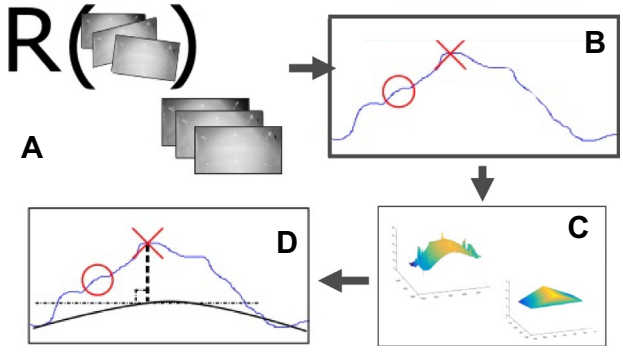

Fig. 3. The 4-step process in computing IVD bulging using the developed computerized algorithm. All images within a specimen condition (Anterior-Intact, Anterior-Reduced or Posterior-Reduced) are aligned to account for any translation that may have occurred relative to the laser when changing between flexed and neutral postures (A), the region of interest for each scan is then selected (B) – the x corresponds to the peak bulge that would be chosen prior to surface reconstruction, whereas the circled portion indicates where the true bulge occurs, the surface curvature of the specific IVD is then estimated (to account for IVD outward bulging in a direction that is not normal to the scanning plane), lastly the point of peak IVD bulge is then computed related to the constructed surface (D).

Anterior-Reduced and Posterior AF bulge measurements, Pearson's r correlation analysis was conducted. Initially, a paired t-test was used to determine if there was a significant difference in the slopes of the posterior-anterior AF bulge comparisons across magnitudes of compressive load. No significant differences were observed and therefore all loading conditions were collapsed into one correlation analysis for each posture.

To examine any potential interactions between load magnitude (10 N, 300 N, 600 N, 1200 N), posture (Flexion, Neutral), and scan location (Anterior-Reduced, Posterior), a 3-way repeated measures general linear model was completed. All statistical analyses were computed using SPSS software (version 9.2, SAS Institute Inc., Cary, NC) with a significance level (α) of 0.05 determined a priori. Tukey post hoc tests were performed on all significant main and interaction effects.

3. Results

Average and Standard Deviation of specimen specific characteristics can be found in Table 1. The removal of the posterior elements from the FSUs resulted in a significant difference in peak AF bulge. On average, there was a 0.11 mm difference (p = 0.012) between the Anterior-Intact and Anterior-Reduced specimens, which occurred due to lower peak AF bulge in the Anterior-Reduced condition.

A significant negative correlation between Anterior-Reduced and Posterior peak AF bulge measurements was observed in a flexed posture (Pearson's r = −0.448; p = 0.002). In flexion, as posterior AF bulge increased, anterior AF bulge decreased. (Fig. 4). No significant correlation was observed between Anterior-Reduced and Posterior AF bulge in a neutral posture (p = 0.312).

A significant 3-way interaction was observed between load magnitude, posture and scan location (p = 0.007). Across load, in flexion, there was significantly more AF bulge on the posterior side in comparison to the anterior side (Fig. 5). In contrast, across all loads, in neutral, there was significantly more AF bulge on the anterior side in comparison to the posterior side (Fig. 4, Table 2).

4. Discussion

Consistent with our hypothesis, results from this investigation elucidate a link between measured AF bulge on the anterior and posterior sides of the IVD, in a flexed posture. The magnitude of posterior AF bulge increased in flexion as the magnitude of the applied compressive load increased. However, no link was observed between AF bulge on the anterior and posterior sides in a neutral posture. In a neutral posture, while not statistically significant, the magnitude of anterior AF bulge slightly increased as the magnitude of applied compressive load increased. Magnitude of compressive load was found to significantly impact peak AF bulge; however, the interaction of posture dictated on which side of the disc this increase occurred.

Results from this investigation revealed a significant difference in AF bulge on the anterior side of the disc across intact and reduced FSUs. Changes in AF bulge across intact and reduced FSUs was expected and aligns with previous work by Heuer and colleagues (2008b), whom showed that removing the posterior structures significantly changed peak AF bulge magnitudes. Heuer and colleagues (2008b), showed that maximum disc bulging increased by approximately 1.4 times, in flexion, when posterior structures were removed. Our results, in contrast, show a slight decrease in peak anterior AF bulge when the posterior elements were removed (0.11 ± 0.44 mm). It is possible that removal of the posterior elements may have resulted in an increase in peak posterior AF bulge, which may account for the decrease in peak

Table 1
Specimen characteristics across C34 and C56 FSUs tested. Computed disc height was measured during the initial intact neutral scan (neutral posture, 300 N compressive load) as the vertical distance between the superior and inferior endplates marked with steel pins. Average intervertebral joint endplate surface area was estimated using the equation of an ellipse and inputted into a regression equation, developed using porcine cervical FSUs, to approximate each specimen's ultimate compressive tolerance (UCT) (Parkinson and Callaghan, 2009). For posture, zero degrees would be parallel to the ground, a negative value indicates extension and positive value indicates flexion.

					Compressive load as a percentage of UCT				Posture (degrees)	
	Specimen type	Disc height (mm) neutral scan	Endplate area (mm^2)	Estimated ultimate compressive tolerance (N)	10 N	300 N	600 N	1200 N	Neutral	Flexion (300% NZ limit)
Average	C34	10.91	665.2	9054.2	0.1%	3.4%	6.8%	13.6%	0.6	8.3
Standard deviation		1.54	110.4	1502.8	0.0%	0.6%	1.2%	2.5%	4.5	6.1
Average	C56	9.63	692.8	9429.9	0.1%	3.2%	6.4%	12.8%	−7.4	−0.7
Standard deviation		0.86	57.0	775.9	0.0%	0.2%	0.5%	1.0%	4.8	4.3

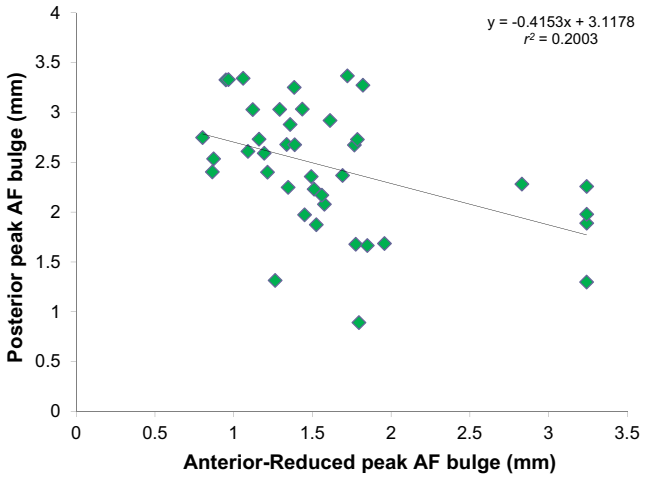

Fig. 4. Scatter plot illustrating a negative correlation between Anterior-Reduced and Posterior AF bulging in a flexed posture.

AF bulge on the anterior side. To obtain an unobstructed view of the posterior side of the disc, the boney posterior structures and posterior longitudinal ligament were removed. The significant negative correlation observed in flexion, between anterior and posterior AF bulge, suggests that as AF bulge increases on the posterior side, AF bulge would decrease on the anterior side. This is one explanation that may elude to the decrease in anterior AF bulge in reduced specimens.

Previous work by Heuer and colleagues (2008b) characterized the effect of posture on AF bulge of the IVD with a 7.5 Nm flexion moment. Results revealed that maximum AF bulge was 2.70 mm and −1.26 mm (inward bulge) on the anterior and posterior sides of the disc, respectively (Heuer et al., 2008b). Similarly, Gooyers and Callaghan (2015) measured peak AF bulge on the anterior side (across all specimens prior to cyclic loading), in porcine specimens, to be 1.35 (0.48) mm, which was less than that reported by Heuer et al. (2008b). Across the specimens that were included in the present study, the average (SD) AF bulge under 300 N and 600 N of compressive load in flexion was 1.70 (0.78) mm and 1.61 (0.64) mm on the anterior side in the Anterior-Reduced condition and 2.49 (0.55) mm and 2.43 (0.54) mm on the posterior side. Such

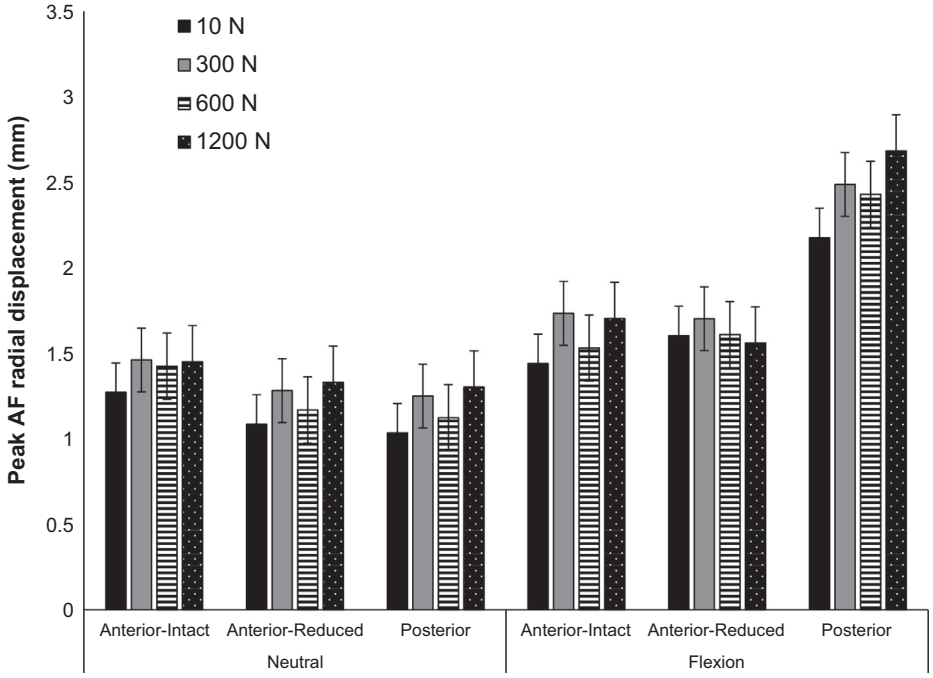

Fig. 5. Average peak AF bulge across experimental conditions for Anterior-Intact, Anterior-Reduced and Posterior conditions. AF bulge Anterior-Intact was not included in the statistical analysis, however, has been included in the figure for reference.

Table 2
Average peak AF bulge across experimental conditions and scan locations. For comparative purposes, average and standard deviation of posture has been reported in degrees, where zero degrees would be parallel to the ground, a negative value indicates extension and positive value indicates flexion.

		Average peak AF bulge (mm)			
Posture	**Scan Location**	**10 N**	**300 N**	**600 N**	**1200 N**
Neutral	Anterior-intact	1.27	1.46	1.43	1.45
(Average = −3.42, SD = 3.78 degrees)	Anterior-reduced	1.09	1.28	1.17	1.33
	Posterior	1.03	1.25	1.12	1.30
Flexion	Anterior-intact	1.44	1.73	1.53	1.70
(Average = 6.07, SD = 6.97 degrees)	Anterior-reduced	1.60	1.70	1.61	1.56
	Posterior	2.18	2.49	2.43	2.69

results are greater than that reported by Gooyers and Callaghan (2015), but less than that reported by Heuer and colleagues (2008) on the anterior side of the disc. However, it is notable that this investigation and the work completed by Heuer and colleagues (2008b) used a reduced specimen, whereas in the work completed by Gooyers and Callaghan (2015) the posterior elements remained intact. In addition, the larger AF bulge observed by Heuer et al. (2008b) may be attributable to the use of human lumbar motion segments, which are approximately 50% greater in size in comparison to porcine FSUs (Yingling et al., 1999).

In this investigation, significantly greater AF bulge was observed on the anterior side of the FSU, in comparison to the posterior side in a neutral posture, which expanded with an increase in compressive load. Heuer et al. (2008a, 2008b), characterized AF bulge of the IVD with 500 N of static compressive force, which is closest to the neutral 600 N condition in this investigation. Heuer et al. (2008b) showed that the maximum outward IVD bulge measured in the posterior-lateral region was approximately 57% of the magnitude measured on the anterior surface (peak outward AF bulge at posterior-lateral region = 0.60 mm, compared to 1.05 mm on the anterior surface) (Heuer et al., 2008b). Results from the current investigation demonstrate a similar trend in neutral, with greater peak outward AF bulge on the anterior side in comparison to posterior in neutral (measured peak bulge on the posterior side was 42% of the magnitude measured on the anterior side).

Across all conditions tested, results from this investigation consistently demonstrated a positive outward AF bulge on the posterior side of the disc. This result conflicts with Heuer et al. (2008b), who consistently reported a negative inward bulge in flexion (range: −1.26 to −0.45 mm) and either a very small outward bulge or inward bulge in neutral (range: −0.07 to 0.60 mm). It is possible that the use of porcine cervical FSU's, which have a gelatinous nucleus pulposus, may have resulted in a different pattern of AF bulging compared to aged human specimens. The inner layers of the IVD have been shown to fold inward resulting in less displacement in older human FSUs (Adams et al., 2000; Yasuma et al., 1990). While the current results are not intended to replicate an *in vivo* loading scenario, results here do align with previous MRI investigation trends that have documented posterior outward IVD bulge (estimates ranging from 1.92 mm to 2.18 mm in healthy human volunteers) in a flexed posture (Fredericson et al., 2001), and 2 mm to 4 mm in human volunteers with grade I to grade V degeneration, respectively (Zou et al., 2009).

It must be acknowledged that the application of findings from this study to the *in vivo* human lumbar spine is limited. First, by the use of porcine cervical FSUs as human surrogates. Secondly, this investigation used a reduced-FSU. The removal of posterior elements and longitudinal ligaments have been shown to influence how the FSU is loaded and thus will likely influence peak AF bulge magnitude and location (Heuer et al., 2008a, 2008b). This investigation was not intended to reflect a clinical scenario but provides new data regarding AF bulging in different regions of the IVD across posture and load. Lastly, time-dependent viscoelastic responses may have occurred throughout the protocol. We attempted to mitigate the influence of this response by, conditioning specimens with the described preload and by randomizing conditions across specimens.

In summary, results from this investigation demonstrate that there is a link between measured AF bulge on the anterior and posterior side of the IVD. Understanding how the AF responds under various loads and postures does have clinical relevance, as IVD herniation has been observed with repeated flexion-extension under modest amounts of compressive load. The magnitude of posterior AF bulge increased in flexion as the magnitude of the applied compressive load increased. Thus, the magnitude of strain and risk of tissue damage in the AF is expected to follow a similar trend.

Declaration of Competing Interest

The authors declare that they have no known competing financial interests or personal relationships that could have appeared to influence the work reported in this paper.

Acknowledgements

The authors would like to acknowledge funding provided by the Natural Sciences and Engineering Research Council of Canada (Grant No. RGPIN-2016-04136). Dr. Jack Callaghan also holds the Canada Research Chair in Spine Biomechanics and Injury Prevention (Tier 1) 950-232134.

References

Adams, M.a., Freeman, B.J.C., Morrison, H.P., Nelson, I.W., Dolan, P., 2000. Mechanical initiation of intervertebral disc degeneration. Spine (Phila. Pa. 1976) 25, 1625–1636. https://doi.org/10.1097/00007632-200007010-00005.

Brinckmann, P., Biggemann, M., Hilweg, D., 1989. Prediction of the compressive strength of human lumbar vertebrae. Spine (Phila. Pa. 1976) 14, 606–610. https://doi.org/10.1097/00007632-198906000-00012.

Callaghan, J.P., McGill, S.M., 2001. Intervertebral disc herniation: studies on a porcine model exposed to highly repetitive flexion/extension motion with compressive force 16, 28–37.

Cuchanski, M., Cook, D., Whiting, D.M., Cheng, B.C., 2011. Measurement of occlusion of the spinal canal and intervertebral foramen by intervertebral disc bulge. SAS J. 5, 9–15. https://doi.org/10.1016/j.esas.2010.09.004.

Fewster, K.M., Haider, S., Gooyers, C.E., Callaghan, J., Wong, A., 2019. A computerised system for measurement of the radial displacement of the intervertebral disc using a laser scanning device. Comput. Methods Biomech. Biomed. Eng. Imaging Vis., 1–7 https://doi.org/10.1080/21681163.2019.1674189.

Fredericson, M., Lee, S.U., Welsh, J., Butts, K., Norbash, A., Carragee, E.J., 2001. Changes in posterior disc bulging and intervertebral foraminal size associated with flexion-extension movement: A comparison between L4–5 and L5–S1 levels in normal subjects. Spine J. 1, 10–17. https://doi.org/10.1016/S1529-9430(01)00014-6.

Gooyers, C.E., Callaghan, J.P., 2015. Exploring interactions between force, repetition and posture on intervertebral disc height loss and bulging in isolated porcine cervical functional spinal units from sub-acute-failure magnitudes of cyclic compressive loading. J. Biomech. 48, 3710–3717. https://doi.org/10.1016/j.jbiomech.2015.08.023.

Haughton, V.M., 1988. MR imaging of the spine. Radiology 166, 297–301. https://doi.org/10.1148/radiology.166.2.3275973.

Heuer, F., Schmidt, H., Wilke, H.-J., 2008a. The relation between intervertebral disc bulging and annular fiber associated strains for simple and complex loading. J. Biomech. 41, 1086–1094. https://doi.org/10.1016/j.jbiomech.2007.11.019.

Heuer, F., Schmidt, H., Wilke, H.J., 2008b. Stepwise reduction of functional spinal structures increase disc bulge and surface strains. J. Biomech. 41, 1953–1960. https://doi.org/10.1016/j.jbiomech.2008.03.023.

Oxland, T.R., Panjabi, M.M., Southern, E.P., Duranceau, J.S., 1991. An anatomic basis for spinal instability: A porcine trauma model. J. Orthop. Res. 9, 452–462. https://doi.org/10.1002/jor.1100090318.

Parkinson, R.J., Callaghan, J.P., 2009. The role of dynamic flexion in spine injury is altered by increasing dynamic load magnitude. Clin. Biomech. 24, 148–154. https://doi.org/10.1016/j.clinbiomech.2008.11.007.

Stokes, I.A., 1988. Bulging of lumbar intervertebral discs: non-contacting measurements of anatomical specimens. J. Spinal Disord. 1, 189–193.

Tampier, C., Drake, J.D.M., Callaghan, J.P., McGill, S.M., 2007. Progressive disc herniation: An investigation of the mechanism using radiologic, histochemical, and microscopic dissection techniques on a porcine model. Spine (Phila. Pa. 1976) 32, 2869–2874. https://doi.org/10.1097/BRS.0b013e31815b64f5.

Thompson, R.E., Barker, T.M., Pearcy, M.J., 2003. Defining the Neutral Zone of sheep intervertebral joints during dynamic motions: an in vitro study. Clin. Biomech. 18 (2), 89–98. https://doi.org/10.1016/S0268-0033(02)00180-8.

Wenger, K.H., Schlegel, J.D., 1997. Annular bulge contours from an axial photogrammetric method. Clin. Biomech. 12, 438–444. https://doi.org/10.1016/S0268-0033(97)00045-4.

Yasuma, T., Koh, S., Okamura, T., Yamauchi, Y., 1990. Histological changes in aging lumbar intervertebral discs. Their role in protrusions and prolapses. J. Bone Jt. Surg. - Ser. A 72, 220–229. https://doi.org/10.2106/00004623-199072020-00009.

Yingling, V.R., Callaghan, J.P., McGill, S.M., 1999. The porcine cervical spine as a model of the human lumbar spine: an anatomical, geometric, and functional comparison. J. Spinal Disord. Tech. 12, 415–423.

Zou, J., Yang, H., Miyazaki, M., Morishita, Y., Wei, F., McGovern, S., Wang, J.C., 2009. Dynamic bulging of intervertebral discs in the degenerative lumbar spine. Spine (Phila. Pa. 1976) 34, 2545–2550. https://doi.org/10.1097/BRS.0b013e3181b3299.